

Dynamical effects of the nanometer-sized polarized domains in $\text{Pb}(\text{Zn}_{1/3}\text{Nb}_{2/3})\text{O}_3$

P. M. Gehring

NIST Center for Neutron Research, National Institute of Standards and Technology, Gaithersburg, Maryland 20899

S.-E. Park*

Materials Research Laboratory, The Pennsylvania State University, University Park, Pennsylvania 16802

G. Shirane

Physics Department, Brookhaven National Laboratory, Upton, New York 11973

(Received 6 November 2000; revised manuscript received 24 January 2001; published 22 May 2001)

Results from an extensive single-crystal neutron-scattering study of the relaxor ferroelectric $\text{Pb}(\text{Zn}_{1/3}\text{Nb}_{2/3})\text{O}_3$ (PZN) in the cubic phase reveal an anomalous ridge of inelastic scattering that extends vertically from the transverse acoustic (TA) branch near 4 meV to the transverse optic (TO) branch near 9 meV at $q \sim 0.2 \text{ \AA}^{-1}$. No zone center optic mode was found. Similar results were recently reported in a sample of PZN doped with 8% PbTiO_3 . We are able to describe the dynamics of this unusual feature using a simple coupled-mode model that assumes the optic mode linewidth $\Gamma_1(q)$ increases sharply near $q = 0.2 \text{ \AA}^{-1}$ as $q \rightarrow 0$. The dramatic increase in $\Gamma_1(q)$ is believed to occur when the wavelength of the optic mode becomes comparable to the size of small polarized nanoregions (PNR) that develop in the cubic phase of PZN, far above $T_c = 410 \text{ K}$. The consequence is that long-wavelength optic modes cannot propagate and become overdamped. Hence the q at which the anomalous scattering is peaked provides an important measure of the size of the PNR. Below T_c , the intensity of this scattering diminishes. At lowest temperatures ($\sim 30 \text{ K}$) the feature is absent, and we observe the recovery of a zone center transverse optic mode near 10.5 meV.

DOI: 10.1103/PhysRevB.63.224109

PACS number(s): 77.84.Dy, 63.20.Dj, 64.70.Kb, 77.80.Bh

I. INTRODUCTION

Scientific research in the field of relaxor ferroelectrics has surged markedly over the past several years. The primary driving force behind the rapid increase in publications in this area has been the observation of an exceptionally large piezoelectric response in single crystals of the two complex perovskite compounds $\text{Pb}[(\text{Mg}_{1/3}\text{Nb}_{2/3})_{1-x}\text{Ti}_x]\text{O}_3$ (PMN- x PT) and $\text{Pb}[(\text{Zn}_{1/3}\text{Nb}_{2/3})_{1-x}\text{Ti}_x]\text{O}_3$ (PZN- x PT) for compositions x that lie near the morphotropic phase boundary (MPB), which separates the rhombohedral and tetragonal regions of the phase diagram. These complex perovskites differ from the classic and well-studied simple ABO_3 -type perovskites by virtue of the mixed-valence character of the B -site cation. In the case of PMN and PZN ($x=0$), the B site is occupied by either Mg^{2+} or Zn^{2+} , and Nb^{5+} ions with a stoichiometry of 1/3 and 2/3, respectively, which is required to preserve charge neutrality. This built-in disorder sharply breaks the translational symmetry of the lattice and produces a so-called “diffuse” phase transition in which the dielectric permittivity ϵ exhibits a large and broad peak at a characteristic temperature T_{max} that is also strongly frequency dependent. In contrast to the normal ferroelectric parent compound PbTiO_3 (PT), in which the condensation of a transverse optic (TO) zone center phonon leads to a transition from a cubic paraelectric phase to a tetragonal long-range ordered state with a non vanishing spontaneous polarization below a critical temperature $T_c = 763 \text{ K}$, the prototypical relaxor compound PMN exhibits a diffuse transition at $T_{\text{max}} = 230 \text{ K}$ and no spontaneous polarization at any temperature studied.

Stimulated by the unusual properties of these complex

systems, we performed a recent neutron-inelastic-scattering study to examine the lattice dynamics of a high-quality single crystal of PZN-8%PT,¹ the composition for which the piezoelectric response is largest in the PZN- x PT system.² The PZN- x PT phase diagram as a function of PT concentration x is shown in Fig. 1. The maximum piezoelectric activity occurs on the rhombohedral side of the MPB, which is indicated by the steep dashed line. Our measurements of the phonon dispersion of the polar TO mode in the cubic phase at 500 K revealed an unexpected ridge of scattering centered

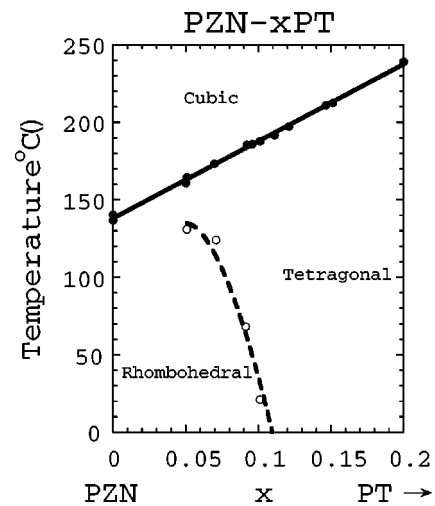


FIG. 1. Phase diagram of the PZN-PT system from Kuwata *et al.* (Ref. 3). The MPB is represented by the dashed line between the rhombohedral and tetragonal phases. An intervening monoclinic phase has been discovered in PZT by Noheda *et al.* (Ref. 4).

at a momentum transfer $q=0.2 \text{ \AA}^{-1}$, measured from the zone center. The ridge extends in energy from ~ 4 to 9 meV such that, when plotted as a standard phonon dispersion diagram, it resembles a waterfall in which the TO branch appears to drop precipitously into the transverse acoustic (TA) branch. This anomalous feature, hereafter referred to as the waterfall, was observed in both of the two Brillouin zones we surveyed $(2,2,l)$, and $(h,h,4)$, which cover the two different symmetry directions $[001]$ and $[110]$. Similar data taken on a large single crystal of pure PMN at room temperature also showed the presence of a waterfall.⁵

The waterfall observed in PZN-8%PT was speculated to represent direct microscopic evidence for small, randomly oriented regions of local polarization within the crystal that begin to condense at temperatures far above $T_c=450$ K. The existence of these regions of local polarization was first proposed by Burns and Dacol in 1983 to describe the disorder inherent to relaxor systems.⁶ Using measurements of the optic index of refraction to study ceramic samples of $(\text{Pb}_{1-3x/2}\text{La}_x)(\text{Zr}_y\text{Ti}_{1-y})\text{O}_3$ (PLZT), as well as single crystals of PMN and PZN,⁶ they discovered that a randomly oriented, and nonreversible local polarization P_d develops at a well-defined temperature T_d , frequently referred to as the Burns temperature, several hundred degrees above the apparent transition temperature T_c . Subsequent studies have provided additional experimental evidence supporting the existence of T_d .⁷⁻⁹ The spatial extent of these locally polarized regions was conjectured to be of the order of several unit cells, and has given rise to the term ‘‘polar nanoregions,’’ or PNR. Because the size of the PNR is finite, the propagation of long-wavelength phonons should be inhibited. This would then lead naturally to a heavily overdamped TO phonon cross section in the neighborhood of the zone center. Indeed, no well-defined TO phonon peaks were found in either PZN-8%PT or PMN for $q < 0.2 \text{ \AA}^{-1}$. Moreover, if one assumes the waterfall peak position in q gives a measure of the size of the PNR according to $2\pi/q$, one obtains a value of 30 \AA , or about 7–8 unit cells, consistent with the conjecture of Burns and Dacol.

Further evidence in support of this picture correlating the waterfall with the appearance of the PNR comes from the neutron inelastic scattering data of Naberezhnov *et al.*¹⁰ As shown in Fig. 2, they observed a normal TO and TA phonon dispersion in the closely related relaxor ferroelectric compound PMN at 800 K $> T_d = 617$ K, where no polar regions remain.¹⁰ However, we studied the same crystal at room temperature, more than 300 K below T_d , and found a prominent waterfall feature. For PZN-8%PT, the formation of the PNR is estimated to occur at $T_d \sim 790$ K, which is well above the cubic-to-tetragonal phase transition at $T_c \sim 450$ K, and also beyond the temperature at which the crystal begins to decompose.

In this paper we present a more complete lattice dynamical study of pure PZN, in which we also observe an anomalous ridge of scattering that closely resembles the waterfall seen in PZN-8%PT and PMN. PZN differs from PMN in that it exhibits an explicit structural phase transformation at 410 K from cubic to tetragonal symmetry. The value of T_{max} for PZN is just slightly above $T_c = 410$ K, and thus much higher

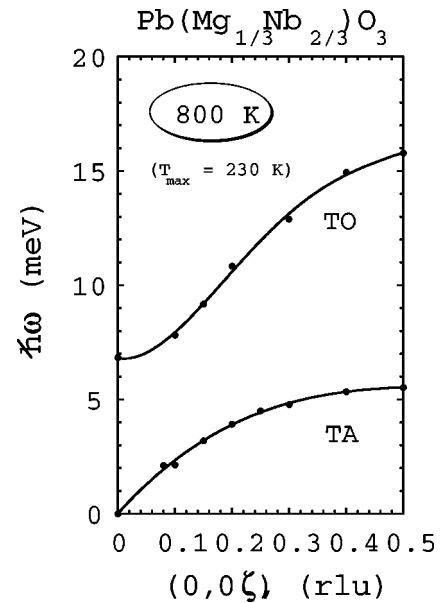


FIG. 2. Dispersion curves of the transverse acoustic (TA) and the lowest-energy transverse optic (TO) modes in PMN measured by Naberezhnov *et al.* (Ref. 10) at 800 K, far above $T_d = 617$ K.

than $T_{\text{max}} = 230$ K for PMN.¹¹ We further present a simple mode-coupling model that clearly relates this unusual feature of the TO phonon branch (the same branch that goes soft at the zone center at T_c in PbTiO_3) to the PNR. Our current study does not, however, cover the critical scattering at small q below 0.075 \AA^{-1} . Extensive studies in this area have already been carried out using neutron¹² and x-ray scattering^{13,14} techniques. As we will show, this is the portion of the Brillouin zone where the TO mode is overdamped because of the PNR.

II. EXPERIMENTAL

Two single crystals of PZN were used in this study, the first, labeled PZN No. 1, weighs 4.2 gr and the second, labeled PZN No. 2, weighs 2.3 gr. Both crystals were grown using the high-temperature flux technique described elsewhere.¹¹ Each crystal was mounted onto an aluminum holder and oriented with the cubic $[001]$ axis vertical, thereby giving access to the $(HK0)$ scattering zone. They were then placed inside a vacuum furnace capable of reaching temperatures of up to 900 K. For temperatures below room temperature, a specially designed closed-cycle helium refrigerator was used to cover the range from 25 to 670 K.

All of the neutron scattering data presented here were obtained on the BT2 triple-axis spectrometer located at the NIST Center for Neutron Research. The (002) reflection of highly oriented pyrolytic graphite (HOPG) was used to monochromate and analyze the incident and scattered neutron beams. An HOPG transmission filter was used to eliminate higher-order neutron wavelengths. The majority of our data were taken holding the incident neutron energy E_i fixed at 14.7 meV ($\lambda_i = 2.36 \text{ \AA}$) while varying the final neutron energy E_f , and using horizontal beam collimations of $60^\circ\text{-}40^\circ\text{-}S\text{-}40^\circ\text{-}40^\circ$ and $60^\circ\text{-}40^\circ\text{-}S\text{-}40^\circ\text{-open}$.

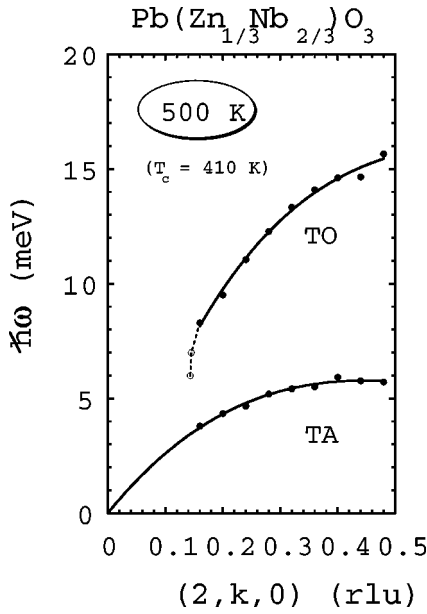


FIG. 3. Solid (open) dots represent positions of peak scattered neutron intensity taken from constant- \vec{Q} (constant- E scans) at 500 K along the cubic [010] symmetry direction in PZN. Solid lines are guides to the eye indicating the TA and TO phonon dispersions.

Two basic types of inelastic scans were used to collect data on each sample. Constant- E scans were performed by holding the energy transfer $\hbar\omega = \Delta E = E_i - E_f$ fixed while varying the momentum transfer \vec{Q} . Constant- \vec{Q} scans were performed by holding the momentum transfer $\vec{Q} = \vec{k}_i - \vec{k}_f$ ($k = 2\pi/\lambda$) fixed while varying the energy transfer ΔE . Using a combination of these scans, the dispersions of both the TA and the lowest-energy TO phonon modes were mapped out at a temperature of 500 K (still in the cubic phase, but well below the Burns temperature for PZN of $T_d \sim 750$ K).

It is worthwhile to note that the high temperature data were taken using neutron energy gain, i.e., by scanning E_f such that the energy transfer $\hbar\omega < 0$. This process is known as phonon annihilation. At high temperatures, and not too large energies, the phonon thermal population factor makes this mode of operation feasible. More importantly, the instrumental energy resolution function contains the factor $\cot 2\theta_a$, where $2\theta_a$ is the analyzer (HOPG) scattering angle. Hence the energy resolution increases with increasing energy because $2\theta_a$ decreases. The net result is an increased neutron count rate at the expense of a broader linewidth, thereby making the relatively weaker transverse optic mode easier to see.

III. INELASTIC SCATTERING DATA FROM PZN NEAR $\vec{Q} = (2, 0, 0)$

The waterfall, previously reported in PZN-8%PT,¹ is shown for PZN No. 1 at 500 K in Fig. 3. The data points represent the peak scattered neutron intensity plotted as a function of $\hbar\omega$ and \vec{q} , where $\vec{q} = \vec{Q} - \vec{G}$ is the momentum transfer relative to the $\vec{G} = (2, 0, 0)$ Bragg reflection, measured along the cubic [010] symmetry direction. The solid

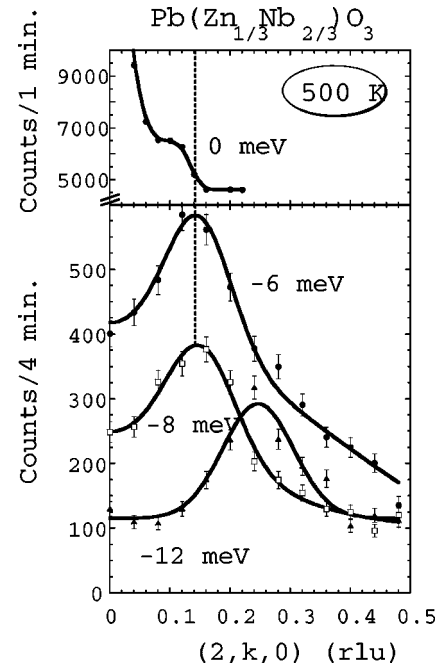


FIG. 4. Constant- E scans at 0, -6, -8, and -12 meV (phonon annihilation) measured at 500 K on PZN crystal No. 1.

dots represent data from constant- \vec{Q} scans whereas the two open circles are data derived from constant- E scans. These latter two data points signal the onset of the waterfall regime in which the TO phonon branch appears to dive into the TA branch, and are thus connected by a dashed line. The lowest-energy data points trace out the TA phonon branch along [010]. Solid lines are drawn through these points as a guide to the eye, and are nearly identical to those shown for PMN in Fig. 2.

As was the case for PZN-8%PT measured at the same temperature, the anomalous ridge of scattering in PZN is approximately centered at 0.14 reciprocal lattice units (rlu) or 0.22 \AA^{-1} ($1 \text{ rlu} = 2\pi/a = 1.545 \text{ \AA}^{-1}$). This is more clearly shown by the series of constant- E scans plotted in Fig. 4 for $\hbar\omega = 0, -6, -8,$ and -12 meV (negative values correspond to phonon annihilation as described above). Both the -6 and -8 meV scans are peaked at the same value of k ($=q$), thereby indicating the presence of the waterfall. The elastic (0 meV) cross-section also appears to exhibit a measurable change in the vicinity of the waterfall q vector, as indicated by the vertical dashed line in Fig. 4. However, this merits further study as the change is small compared to the sizable background present due to scattering from the aluminum sample holder. If it is real, this observation would suggest that the effects of the PNR extend in energy all the way from the TO branch through the TA branch and into the elastic channel. The -12 meV scan, by contrast, peaks at a larger momentum transfer q (~ 0.24 rlu) that lies outside the waterfall regime, and instead represents a genuinely propagating TO phonon mode.

Peaks in constant- E scans do not guarantee propagating modes. This can only be confirmed using constant- \vec{Q} scans. Therefore we show four representative constant- \vec{Q} scans in

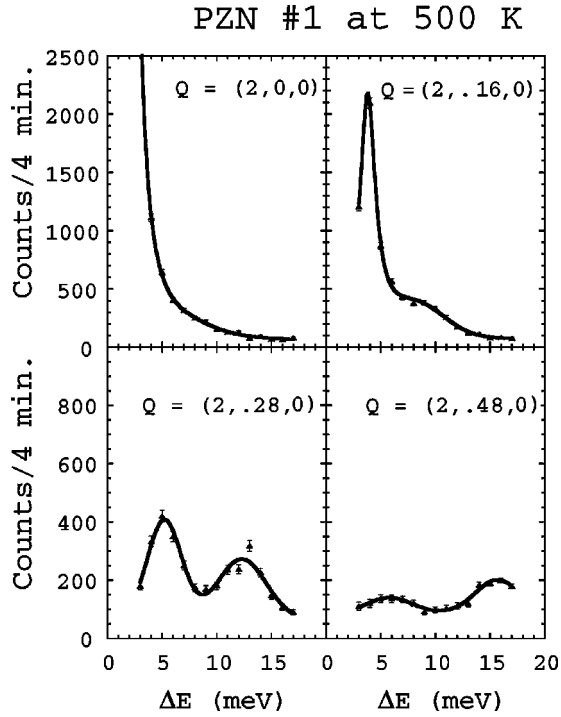


FIG. 5. Constant- \vec{Q} scans at 0.00, 0.16, 0.28, and 0.48 rlu measured at 500 K on PZN crystal No. 1.

Fig. 5 for the q values 0.00, 0.16, 0.28, and 0.48 rlu. For $q > 0.16$ rlu, two distinct peaks are present, corresponding to the TA and TO phonon modes. At 0.16 rlu, one sees the TO mode beginning to become damped while the intensity of the TA mode has become relatively much more intense. For $q < 0.16$ rlu, the TA mode was indistinguishable from the elastic peak. Most striking is the absence of any peak in the constant- \vec{Q} scan for $q = 0.00$ rlu. There is no clear peak for the TO mode for $q < 0.16$ rlu, indicating that these polar optic modes are heavily overdamped.

To illustrate this behavior as clearly as possible, a series of constant- \vec{Q} scans were collected in steps of 0.04 rlu along $(2, k, 0)$ that spanned the entire Brillouin zone. After subtraction of a constant background, the data have been plotted as a contour plot in Fig. 6. For ease of comparison, the contour plot has been drawn with the same vertical and horizontal scales used in Figs. 2 and 3. At large q near the zone boundary, the TO and TA phonon branches are readily apparent as broad green features. Near the waterfall regime, the TO branch appears to drop almost vertically into the TA branch with a corresponding increase in intensity. Below $q \sim 0.14$ rlu, the intensity contours show no peak (scanning vertically) that could correspond to a propagating mode. The acoustic mode looks to be flat below 4 meV only because the color scale covers a limited intensity range above which all data are colored yellow. The intensity range was limited on purpose to make the waterfall feature more visible. Even so, one can notice a rapid increase in the TA phonon intensity in the vicinity of the waterfall, suggesting that a transfer of intensity might be occurring between the TO and TA modes. To examine this possibility, we performed model calcula-

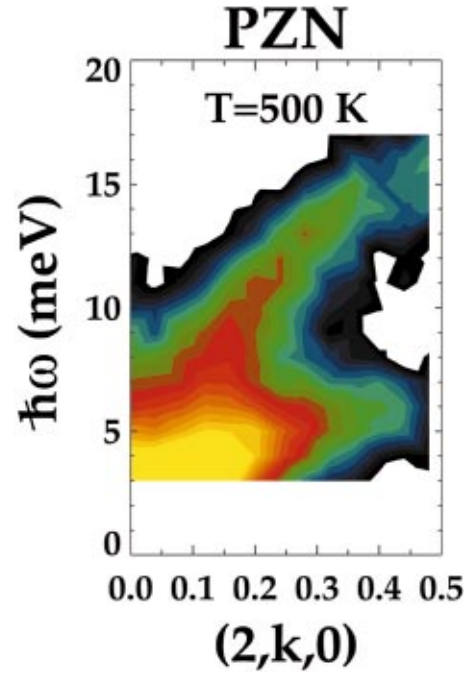


FIG. 6. (Color) Contour map of the background subtracted scattering intensity from PZN at 500 K measured near (200) . The intensity data are represented on a logarithmic color scale with yellow representing the highest intensity, and black the lowest, and are limited to a narrow range in order to better show the waterfall.

tions using a simple mode-coupling scheme to simulate the anomalous features reported here in the PZN compound.

IV. MODE-COUPLING MODEL

During the course of our experiments on relaxor ferroelectrics, a simple but effective model describing the anomalous low-frequency lattice dynamics was developed assuming a coupling between the TO and TA phonon modes. For the case of neutron energy loss, the scattering intensity distribution I for two interacting modes with frequencies Ω_1 and Ω_2 , and widths Γ_1 and Γ_2 , is given by the expression¹⁵

$$I \sim [n(\omega) + 1] \frac{\omega}{A^2 + \omega^2 B^2} \{ [(\Omega_2^2 - \omega^2)B - \Gamma_2 A] F_1^2 + 2\lambda B F_1 F_2 + [(\Omega_1^2 - \omega^2)B - \Gamma_1 A] F_2^2 \}, \quad (1)$$

where A and B are given by

$$A = (\Omega_1^2 - \omega^2)(\Omega_2^2 - \omega^2) - \omega^2 \Gamma_1 \Gamma_2, \quad (2)$$

$$B = \Gamma_1(\Omega_2^2 - \omega^2) + \Gamma_2(\Omega_1^2 - \omega^2),$$

and $n(\omega)$ is simply the Bose factor $[e^{(\omega/k_B T)} - 1]^{-1}$. The quantities $F_{1,2}$ are the structure factors of modes 1 and 2, and λ is the coupling strength between the two modes. Extensive model calculations based on this equation, which describes the behavior of coupled-phonon cross sections quite well,^{15,16} have been performed in collaboration with Ohwada at the Institute of Solid State Physics, University of Tokyo.¹⁷

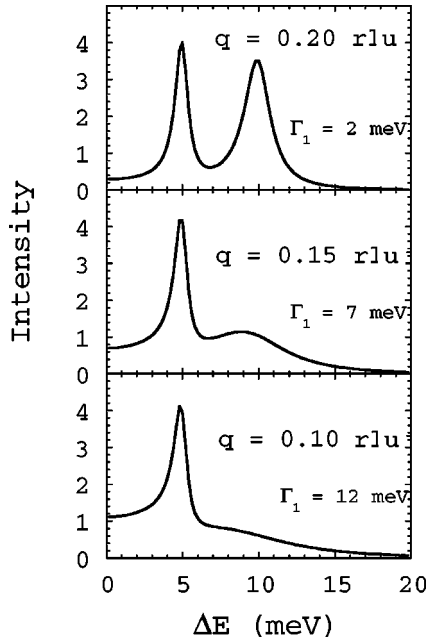


FIG. 7. Model simulations assuming a coupled-mode intensity distribution and a strongly q -dependent TO phonon linewidth Γ_1 . Three constant- \bar{Q} scans are shown corresponding to $q=0.20$, 0.15 , and 0.10 rlu, with $q=0.15$ rlu taken to be the reciprocal space position of the anomalous waterfall feature.

The essential physics behind the mode-coupled model description of the waterfall is built into the linewidth of the TO mode Γ_1 , which is assumed to become sharply q dependent as the polar nanoregions begin to form at the Burn's temperature T_d . If we suppose that the PNR have an average diameter given by $2\pi/q_{wf}$, where q_{wf} represents the reciprocal space position of the waterfall, then those optic phonons having $q < q_{wf}$ will not be able to propagate easily because their wavelength exceeds the average size of the PNR. These polar lattice vibrations are effectively impeded by the boundary of the PNR. This idea has also been discussed by Tsurumi *et al.*¹⁸ The simplest way to simulate this situation is to assume a sudden and steep increase in $\Gamma_1(q)$ at q_{wf} . For this purpose, a Fermi-distribution function of q works extremely well. Figure 7 shows several model constant- \bar{Q} simulations based on this assumption, using the values $q_{wf}=0.15$ rlu, $\lambda=10$, $F_1=4$, $F_2=1$, and $\Gamma_2=1$. For simplicity and purposes of illustration, the dispersions of both optic and acoustic modes were ignored by holding the parameters $\Omega_{1,2}$ fixed at 10 and 5 meV, respectively, over the entire Brillouin zone. Similarly, instrumental resolution effects were not included.

For $q > q_{wf}$ one observes two broad peaks, as expected. At momentum transfers $q < q_{wf}$, however, the optic mode becomes highly overdamped and its profile extends in energy below that of the acoustic mode. Alongside each constant- \bar{Q} scan is shown the corresponding value of Γ_1 used in the simulation. The waterfall thus represents the crossover between a high- q regime, in which one observes two well-defined peaks corresponding to two propagating modes, and a low- q regime, in which one observes an overdamped optic

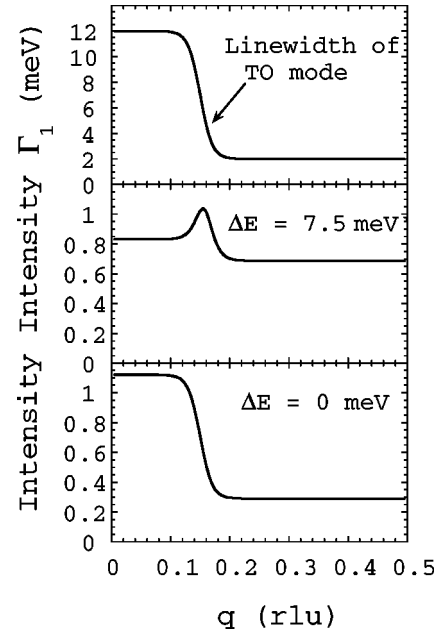


FIG. 8. Model simulations of two constant- E scans at 0 and 7.5 meV. The q dependence of the TO linewidth Γ_1 is shown in the top panel for ease of comparison.

mode plus an acoustic peak. This simple model cross section describes all of the experimental observations very well. Indeed, one can favorably compare the simulated scan at $q=0.15$ rlu in Fig. 7 with the experimental scan for $\bar{Q}=(2,0,16,0)$ shown in Fig. 5. One can see now that the waterfall is *not* a TO phonon dispersion at all. Instead, it is simply a redistribution of the optic mode profile that is caused by the PNR which force a sudden change in the optic mode linewidth at a specific q related to the average size of the PNR.

To illustrate the salient features of the scattering cross-section within the coupled-mode model, the q dependence assumed for the optic mode linewidth Γ_1 is shown in Fig. 8 along with two constant- E scans calculated for 0 and 7.5 meV. The sharp increase in Γ_1 has a corresponding and pronounced effect on both cross-sections in the vicinity of q_{wf} . The extreme broadening of the TO mode that occurs near q_{wf} causes a redistribution of the scattering underneath the TA mode and into the elastic channel. Because of the sum rule for the energy-integrated scattering, a compensatory jump occurs in the elastic cross section. The size of this jump depends on the energy scale of the increase in Γ_1 . We note that despite the fact that no resolution effects, background, or Bragg terms were included in these calculations, the agreement with experiment is surprisingly good. Indeed, the cross section calculated for 0 meV is striking in its similarity to the experimentally measured elastic cross section shown in the top panel of Fig. 4, and thus lends credence to the coupled-mode model.

V. TEMPERATURE DEPENDENCE

Our data on the temperature dependence of the waterfall in PZN are limited because PZN decomposes at a tempera-

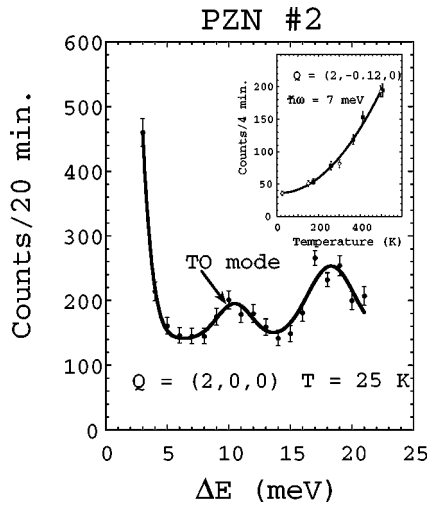


FIG. 9. Constant- \vec{Q} scan at $(2,0,0)$ and 25 K taken on PZN crystal No. 2 showing the recovery of the TO zone center mode at low temperature. The inset gives the temperature dependence of the raw scattering intensity measured at $\vec{Q} = (2, -0.12, 0)$ at 7 meV (no background subtraction).

ture less than the Burns temperature. This prevents us from performing measurements above T_d which would have allowed us to monitor the recovery of zone center and low- q TO phonons at temperatures where the polarized nanoregions no longer exist. PMN, by contrast, has a lower T_d . Hence, Naberezhnov *et al.* were able to measure the TO phonon dispersion at 800 K $> T_d$ where they observed a normal TO phonon branch.¹⁰ Selected phonons were briefly studied at 860 K in PZN-8%PT.¹ There the scattering intensity associated with the waterfall increased (as expected from the Bose temperature factor) beyond that measured at 500 K, and the peak position of the waterfall, measured using constant- E scans, shifted in towards the zone center, i.e., from $(2,0.14,0)$ to $(2,0.10,0)$. Constant- \vec{Q} data at $(2,0.10,0)$ show a broad peak around 10 meV. These data suggest that around 860 K the PNR have already begun to form inside the “uniform,” or unpolarized crystal. A complete understanding of the behavior in this temperature range must await further study of PMN.

Below the PZN tetragonal-to-rhombohedral phase transition at 410 K the scattering intensity associated with the waterfall decreases gradually, and is almost completely gone at 100 K. This behavior is summarized in the inset to Fig. 9 where the raw intensity (no background subtraction) at $\vec{Q} = (2, -0.12, 0)$ and $\hbar\omega = 7$ meV is plotted versus temperature. Figure 9 itself is a constant- \vec{Q} scan at $(2,0,0)$ and 25 K which clearly shows the presence of a zone center TO mode.

VI. DISCUSSION

We have discovered an anomalous ridge of inelastic scattering that is peaked roughly 0.2 \AA^{-1} from the zone center in the relaxor ferroelectric compound PZN in the cubic phase at 500 K. Similar features were observed previously in the PZN-8%PT, and PMN systems, also in their respective cubic phases. This scattering was observed in various different Brillouin zones including (220) and (004) in PZN-8%PT, and (200) , (300) , and (220) in PZN. The ridge of scattering is extended in energy in such a way as to make the lowest-lying TO phonon branch appear to drop precipitously into the TA phonon branch at a specific value of q , thereby resembling a waterfall. Equally important is the manifestation of a significant change in the elastic cross section near the same value of q . An unusual feature has also been observed by Lushnikov *et al.* for pure PMN using Raman and neutron inelastic scattering techniques at 77 K over an extended energy range from 5.2 to 6.8 meV, which nearly coincides with that of the waterfall feature reported here.¹⁹ This was interpreted as evidence of a fracton, i.e., an excitation on a fractal lattice. We have shown that a simple coupled-mode model can be used effectively to describe our neutron inelastic data by postulating a sharply q -dependent TO phonon linewidth Γ_1 that exhibits a large steplike increase with decreasing q upon reaching the waterfall wave vector q_{wf} . In this way we are able to relate the waterfall directly to the presence of nanometer-sized polarized nanoregions in the crystal which serve to damp the polar TO modes at low q . We speculate that this feature may be common to all relaxor systems in which PNR are present, and further that q_{wf} can provide a measure of the size of the PNR. We hope that our results will stimulate theoretical calculations of the precise q dependence of Γ_1 to allow for quantitative comparison with experiment. It will be interesting to investigate the effects of an applied electric field E on the waterfall, and we have already begun measurements to this end.

ACKNOWLEDGMENTS

We would like to thank Y. Fujii, K. Hirota, B. Noheda, K. Ohwada, S. B. Vakrushev, G. Yong, and H. D. You for stimulating discussions. Financial support by the U. S. Dept. of Energy under Contract No. DE-AC02-98CH10886, by the Office of Naval Research under project MURI (N00014-96-1-1173), and under resource for piezoelectric single crystals (N00014-98-1-0527) is acknowledged. We also acknowledge the support of the NIST Center for Neutron Research, U. S. Dept. of Commerce, in providing the neutron facilities used in this work.

*Present address: Fraunhofer-IBMT Technology Center Hialeah, Hialeah, Florida 33010.

¹P.M. Gehring, S.-E. Park, and G. Shirane, Phys. Rev. Lett. **84**, 5216 (2000).

²S.-E. Park and T.R. Shrout, J. Appl. Phys. **82**, 1804 (1997).

³J. Kuwata, K. Uchino, and S. Nomura, Ferroelectrics **37**, 579

(1981); Jpn. J. Appl. Phys. **21**, 1298 (1982).

⁴See, for example, B. Noheda, D.E. Cox, G. Shirane, J.A. Gonzalo, L.E. Cross, and S.-E. Park, Appl. Phys. Lett. **74**, 2059 (1999).

⁵P. M. Gehring, S. B. Vakrushev, and G. Shirane, in *Fundamental Physics of Ferroelectrics 2000*, edited by R. E. Cohen

- (American Institute of Physics, Melville, NY, 2000), Vol. 535, p. 314.
- ⁶G. Burns and F.H. Dacol, *Phys. Rev. B* **28**, 2527 (1983); *Solid State Commun.* **48**, 853 (1983).
- ⁷N. de Mathan, E. Husson, G. Calvarin, J.R. Gavarri, A.W. Hewat, and A. Morell, *J. Phys.: Condens. Matter* **3**, 8159 (1991).
- ⁸A.A. Bokov, *Ferroelectrics* **131**, 49 (1992).
- ⁹J. Zhao, A.E. Glazounov, Q.M. Zhang, and B. Toby, *Appl. Phys. Lett.* **72**, 1048 (1998).
- ¹⁰A. Naberezhnov, S. Vakhrushev, B. Dorner, and H. Moudden, *Eur. Phys. J. B* **11**, 13 (1999).
- ¹¹S.-E. Park, M.L. Mulvihill, G. Risch, and T.R. Shrout, *Jpn. J. Appl. Phys., Part 1* **36**, 1154 (1997).
- ¹²S. Vakhrushev, A. A. Naberezhnov, N.M. Okuneva, and B.N. Savenko, *Phys. Solid State* **37**, 1993 (1995).
- ¹³S. Vakhrushev, A. Naberezhnov, S.K. Sinha, Y. P. Feng, and T. Egami, *J. Phys. Chem. Solids* **57**, 1517 (1996).
- ¹⁴H. You and Q.M. Zhang, *Phys. Rev. Lett.* **79**, 3950 (1997).
- ¹⁵M. Bullock, J. Zarestky, C. Stassis, A. Goldman, P. Canfield, Z. Honda, G. Shirane, and S.M. Shapiro, *Phys. Rev. B* **57**, 7916 (1998).
- ¹⁶J. Harada, J.D. Axe, and G. Shirane, *Phys. Rev. B* **4**, 155 (1971).
- ¹⁷K. Ohwada (private communication).
- ¹⁸T. Tsurumi, K. Soejima, T. Kamiya, and M. Daimon, *Jpn. J. Appl. Phys., Part 1* **33**, 1959 (1994).
- ¹⁹S.G. Lushnikov, S.N. Gvasaliya, and I.G. Siny, *Physica B* **263-264**, 286 (1999).